Genomics 113 (2021) 2756–2768

Contents lists available at ScienceDirect

Genomics

journal homepage: www.elsevier.com/locate/ygeno

Original Article

Evolutionary history and functional characterization of *Lj-TICAM-a* and *Lj-TICAM-b* formed via lineage-specific tandem duplication in lamprey (*Lampetra japonica*)

Ming Geng [a,b,c,1], Yishan Hua [a,b,c,1], Yu Liu [a,b,c], Jian Quan [a,b,c], Xueting Hu [a], Peng Su [a,b,c], Yingying Li [a,b,c], Xin Liu [a,b,c], Qingwei Li [a,b,c,*], Ting Zhu [a,b,c,*]

[a] College of Life Sciences, Liaoning Normal University, Dalian 116081, China
[b] Lamprey Research Center, Liaoning Normal University, Dalian 116081, China
[c] Collaborative Innovation Center of Seafood Deep Processing, Dalian Polytechnic University, Dalian 116081, China

ARTICLE INFO

Keywords:
Toll-like receptor
TICAM-a
TICAM-b
Evolution
Innate immunity
Lamprey

ABSTRACT

Toll/interleukin-1 receptor domain-containing adaptor molecule (*TICAM*) genes respond to infections. We identified *TICAM-a* and *TICAM-b* in *Lampetra japonica* and investigated their evolutionary history and potential function via comparative genomics and molecular evolution analyses. They are arranged in tandem and evolved from a multi-exon to a single-exon structure. *Lj-TICAM-a* and *Lj-TICAM-b* might be the ancestral gene of the vertebrate *TICAM* genes. *Lj-TICAM-b* arose via a lamprey-specific tandem duplication event. Both genes are expressed in many tissues during an immune response, and exhibit different responses to peptidoglycan, indicating their functional divergence. Simultaneous overexpression of both proteins activated nuclear factor κB expression and co-immunoprecipitation assays indicated that they might form a complex for signal transduction. However, unlike in mammals, the TICAM-dependent signaling pathway in lamprey might rely on TRAF3 rather than on TRAF6. These results suggest that both *Lj-TICAM-a* and *Lj-TICAM-b* play a role in host defenses.

1. Introduction

Pattern recognition receptors (PRRs) play an important role in host cell recognition and defense against microbial pathogens by the innate immune system. PRRs, including Toll-like receptors (TLRs), recognize pathogens based on pathogen-associated molecular patterns (PAMPs) [1–4]. To date, five mammalian Toll/interleukin-1 receptor (TIR) domain-containing adaptors: namely, myeloid differentiation primary response 88 (MyD88), sterile and armadillo motif-containing protein (SARM), TIR domain-containing adaptor protein (TIRAP, also known as MAL), TIR domain-containing molecule 1 (TICAM-1, also known as TRIF), and TIR domain-containing molecule 2 (TICAM-2, also known as TRAM) [5–7], have been described. Although TICAM-1 and TICAM-2 were discovered later than others, they are two crucial adaptors involved in MyD88-independent pathway, which is thought to be a vertebrate innovation.

Conserved in all TLRs, intracytoplasmic TIR domains, are involved in TLR signaling pathways. TIR domain-containing adaptors mediate TLR signaling specificity. Following pathogen recognition via TLR, MyD88-dependent and TICAM-dependent signaling cascades are activated based on the adaptors present. MyD88, a universal adaptor protein that recognizes all TLRs except TLR3, has been found to be highly conserved during species evolution [5]. SARM inhibits TICAM-1-dependent TLR3 and TLR4 signaling and MyD88-dependent pathway [8]. TIRAP participates in MyD88-dependent-TLR2 and MyD88-dependent-TLR4 signaling pathways, by acting as a bridge to recruit MyD88, thus activating nuclear factor κB (NF-κB) [9,10]. Of note, TLR2 senses gram-positive bacteria, and TLR4 senses gram-negative bacteria. TICAM-1 is a key adaptor molecule that relies on the TICAM signaling pathway activated by TLR3 or TLR4. TLR3 specifically recognizes viral dsRNA and its analog, polyinosinic–polycytidylic acid (Poly I:C). Hence, the TLR3-TICAM-1-mediated signaling pathway is one of the most important immune pathways that act against RNA viral infections [11]. TLR4 can recruit TICAM-2 only in the absence of TICAM-1, but it can recruit TICAM-1 even in the presence of TICAM-2 [12]. The interaction of TICAM-1 and TICAM-2 with TLR upregulates interferon (IFN) β,

* Corresponding authors at: College of Life Sciences, Liaoning Normal University, Dalian 116081, China.
E-mail addresses: liqw@263.net (Q. Li), zhut@lnnu.edu.cn (T. Zhu).
[1] Ming Geng and Yishan Hua contributed equally to this work.

https://doi.org/10.1016/j.ygeno.2021.06.022
Received 7 July 2020; Received in revised form 6 May 2021; Accepted 6 June 2021
Available online 18 June 2021

activator protein 1 (AP-1), and NF-κB [13,14]. In vertebrates, tumor-necrosis factor (TNF) receptor-associated factors (TRAFs) are involved

ExPASy (http://www.expasy.org/tools/scanprosite). The molecular weight and isoelectric point (pI) were predicted by ProtParam (https://web.expasy.org/protparam/). The subcellular localization of proteins was predicted by PSORT II (https://psort.hgc.jp/form2.html). TIR domains were identified using PFAM (http://pfam.sanger.ac.uk/search) and SMART (http://smart.embl-heidelberg.de/) databases. For sequence alignments and phylogenetic analysis, the amino acid sequences of TICAM proteins and other three types of TIR-containing adaptors (MyD88, SARM and TIRAP/MAL) were obtained from the NCBI (http://www.ncbi.nlm.nih.gov/). Accession numbers for all sequences used in this study were listed in Supplementary Table S1. Multiple sequence alignments were performed using MUSCLE [42] in MEGA X software [43] with default settings. The neighbor-joining (NJ) tree and maximum likelihood (ML) tree based on the most appropriate model were constructed using MEGA X [43] with 1000 bootstrap replicates. The TICAM motifs were predicted using MEME version 5.0.5 (http://meme-suite.org/tools/meme), with motif size ranging between 6 and 50 amino acids and a maximum of 10 motifs per protein sequence.

2.4. Prediction of gene structure and analysis of genomic collinearity

The genomic sequences used for the analysis of gene structure and gene collinearity of lamprey *TICAM-a* and *TICAM-b* were obtained from the L. *reissneri* genome. The published sea lamprey and Japanese lamprey genomes were also used for verification. Gene structure information (exons and introns) for other species was downloaded from Ensembl database (http://asia.ensembl.org/index.html). The genetic structure of *TICAM-a* and *TICAM-b* was predicted using Gene Structure Display server (http://gsds.cbi.pku.edu.cn/). The genetic information of *TICAM* genomic fragments in each species was obtained from Genomicus v92.01 (http://www.genomicus.biologie.ens.fr) and validated on the Ensembl database to increase accuracy.

2.5. PAMP challenge, tissue sampling, and real-time quantitative PCR

The 48 lampreys were equally allocated into 16 groups and separately injected (abdominal cavity injection) with 100 μL of 1 μg/μL solutions of polyinosinic–polycytidylic acid (Poly I:C), lipopolysaccharide (LPS), and peptidoglycan (PGN) in phosphate-buffered saline (PBS), for 4, 8, 24, and 48 h. The non-challenged control was treated with PBS. The stimulants were purchased from Sigma (St. Louis, MO, USA). Liver, kidney, supraneural body, gill, leukocytes, intestine, and heart tissue samples were extracted from three healthy L. *japonica* adults. Hearts were extracted from another injected L. *japonica* adult. Total RNA was extracted from each lamprey tissue sample using TRIzol (Invitrogen, Carlsbad, CA, USA), and reverse transcription was performed with a PrimeScript RT-PCR kit (TaKaRa) [44], as previously described [45].

Real-time quantitative PCR (RT-qPCR) was used to evaluate the expression of *Lj-TICAM-a* and *Lj-TICAM-b* in different lamprey tissues. *GAPDH* (GenBank accession No. KU041137.1) was used as an internal control [46]. Primers specific for *GAPDH*, *Lj-TICAM-a*, and *Lj-TICAM-b* were synthesized by Sangon (Table 1). RT-qPCR was conducted using the SYBR PrimeScript RT-PCR Kit (Vazyme Biotech Co., Ltd), according to the manufacturer s protocol. The RT-qPCR reaction contained 10 μL Master Mix, 8.2 μL ddH_2O, 0.4 μL upstream primer (10 μmol/L), 0.4 μL downstream primer (10 μmol/L), and 1 μL cDNA (2 μg/μL). The RT-qPCR cycling conditions were: initial denaturation at 95 °C for 30 s; followed by 40 cycles of 5 s at 95 °C, 30 s at 60 °C, and 30 s at 72 °C. Thermal Cycler Dice real-time system analysis software was used to perform three repeated analyses on each sample. The specificity of the RT-qPCR reaction was verified by melting curve analysis.

2.6. Transient transfection and dual-luciferase reporter assay

Plasmids pEGFP-C1-Lj-TICAM-a and pcDNA3.1-N1-HA-Lj-TICAM-b were propagated and extracted from a culture of *E. coli* using the MiniBEST Endo-free Plasmid Purification Kit (TaKaRa). The plasmid concentration was at least 0.5 μg/μL. HEK293T cells were plated in 96-well plates (1×10^6 cells per well) (Jet Bio-Filtration, Guangzhou, China) 24 h before transfection at a cell fusion rate of 70–80%. Transfection was performed according to the instructions of the manufacturer using Lipofectamine 3000 (Invitrogen, USA). Four groups were prepared, each of which was transfected with 0 (control group), 50, and 100 ng test plasmid. The amount of pNF-κB-luc plasmid was 100 ng/well. The phRL-TK reference plasmid was added at a ratio of 10:1. When lower volumes of plasmid were used, the remainder of the system was complemented w 0 b g tA b lasr

TICAM-b) or empty plasmids. Then, at 24 h post-transfection, whole-cell extracts were prepared in 400 μL RIPA buffer (Beyotime) with a cocktail of protease and phosphorylase inhibitors (Beyotime). The protein concentration in the control and experimental groups was determined by the BCA protein assay kit and β-Actin (1: 2000; Abmart, Shanghai, China) antibody as the internal reference. An equal volume of the total cell lysate from each condition was resolved by 10% SDS PAGE and analyzed by western blotting. TRAF3 (1:2000), TRAF6 (1:2000), NF-κB-P65 (1:2000), phospho-NF-κB-p65 (Ser536) (1:1000), and phospho-IKB (Ser32/Ser36) (1:1000) antibodies were obtained from Proteintech Group (Wuhan, China).

2.8. Statistical analysis

All statistical analyses were performed using GraphPad Prism 7.0 software. The western blot data were analyzed by ImageJ. Differences between treatment groups were determined by two-way ANOVA. The value of $P < 0.05$ was set as the significance threshold (*P < 0.05, **$P <$ 0.01, ***$P < 0.001$). Bar charts show the mean ± standard deviation (SD) of three independent experiments.

3. Results

3.1. Identification, molecular cloning, and sequence analysis of Lj-TICAM-a and Lj-TICAM-b

The *P. marinus* [39], *L. reissneri* [40], and L. *japonica* [41] genomes have been published. To comprehensively identify *TICAM* genes, human and zebrafish protein sequences were used as queries for BLAST-search against the high-quality chromosome-level genome assembly of L. *reissneri*, which has higher integrity and continuity than previously published sea lamprey and Japanese lamprey genomes. Ultimately, *Lj-TICAM-a* (GenBank accession no. **MT591270**) and *Lj-TICAM-b* (GenBank accession no. **MT591271**) were cloned using primers designed based on the *L. reissneri* genome sequences.

The *Lj-TICAM-a* ORF is 2376 bp long and encodes a 791-amino acid protein (Fig. S1A) with a predicted molecular mass of 85.07 kDa and a theoretical pI of 5.49. The *Lj-TICAM-b* ORF is 1242 bp long and encodes a 413-amino acid protein (Fig. S1B) with a predicted molecular mass of the encoded protein is 47.00 kDa and a theoretical pI of 6.21. Neither protein has a signal peptide or transmembrane domains (Fig. S2A). SMART predictive analysis of protein domains revealed that Lj-TICAM-a and Lj-TICAM-b contain the typical domain of TLR adaptor proteins, the TIR domain (Fig. S2B). PSORT II software prediction of subcellular localization indicated that Lj-TICAM-a and Lj-TICAM-b are highly likely to be located in the nucleus.

3.2. Phylogenetic tree and conserved protein domain analysis of Lj-TICAM-a and Lj-TICAM-b

To explore the evolutionary relationships of lamprey TICAM-a/b and other TIR-containing adaptors, especially the jawed vertebrate TICAM-1 and TICAM-2, the NJ and ML phylogenetic trees were built (Fig. 1 and Fig. S3) using 76 full-length protein sequences from all five types of TIR-containing adaptors. According to the phylogenetic trees, the different types of TIR-containing adaptors, including MyD88, SARM, TIRAP/MAL, and TICAM, form a monophyletic group, respectively. Vertebrate TICAM-1 and TICAM-2 share a closed evolutionary relationship, and lamprey TICAM-a and TICAM-b are placed at the base of the vertebrate TICAM clade. Therefore, we hypothesize that the lamprey TICAM-a and TICAM-b are likely the co-orthologs of jawed vertebrate TICAM-1 and TICAM-2.

3.3. Multiple-sequence alignment and MEME motif prediction for the TICAM family

Multiple alignments and amino acid sequence similarity comparison of Lj-TICAM-a and Lj-TICAM-b with TICAM from other species are shown in Fig. S4. The comparison revealed some important points regarding the relationship between Lj-TICAM-a and Lj-TICAM-b, and mammalian TICAM-1 and TICAM-2. Shark Cm-TICAM-1 and Cm-TICAM-2 shared higher sequence similarity with vertebrate TICAM-1 and TICAM-2, respectively, than with lamprey TICAM-a and TICAM-b. Fig. S4 shows important homologous sites within vertebrate TICAM-1 and TICAM-2. These results illustrated that shark TICAM proteins clearly differentiated into TICAM-1 and TICAM-2. Furthermore, Lj-TICAM-a and Lj-TICAM-b lack the TRAF6 binding motif (amino acids 250–256, the numbering is based on Hs-TICAM-1, also described below). However, Lj-TICAM-a has the RHIM binding motif (amino acids 651–689). In addition, known important sites of TICAM-2, such as the membrane-binding sites (amino acid 2, amino acids 7–8, the numbering is based on Hs-TICAM-2, also described below), phosphorylation sites (amino acids 6–7 and 15–16), potential TRAF2 binding sites (amino acids 195–200), and potential ERK phosphorylation sites (amino acids 187–188) are missing in both Lj-TICAM-a and Lj-TICAM-b. This implied that the functions of lamprey TICAM proteins are different from those of vertebrate TICAM proteins, and that the functional sites of Lj-TICAM-a and Hs-TICAM-1 are relatively similar. The similarities shared by the TIR domains of Lj-TICAM-a, Lj-TICAM-b, Hs-TICAM-1, and Hs-TICAM-2 were calculated based on the comparison of TIR domains. Lj-TICAM-a shared a similarity of 59.1% with Hs-TICAM-1 and 56.9% with Hs-TICAM-2, while Lj-TICAM-b shared a similarity of 55.9% with Hs-TICAM-1 and 50.5% with Hs-TICAM-2. Taken together, these results showed that Lj-TICAM-a and Lj-TICAM-b are both more similar to Hs-TICAM-1 than to Hs-TICAM-2.

The MEME website was used to predict the TICAM motifs in multiple species, including lamprey, and to analyze the evolutionary characteristics of the secondary structure of Lj-TICAM-a and Lj-TICAM-b (Fig. 2). In addition, motif differences between Lj-TICAM-a and Lj-TICAM-b, and vertebrate TICAM-1 and TICAM-2 were analyzed. The analysis revealed that TICAM-1 contains motifs 1, 3–6, 8 and 10; TICAM-2 contains motifs 4 and 6–8, which forms the TIR domain with Lj-TICAM-a/b; and Lj-TICAM-a and Lj-TICAM-b contain motifs 4 and 6–8, similar to TICAM-2. Additionally, motifs 6–8, 10 were detected in all TICAM sequences, suggesting that they are the most primitive and conserved functional motifs of TICAM family. Together, our observations further support the hypothesis that lamprey TICAM-a/b represent the ancient co-ortholog of vertebrate TICAM-1 and TICAM-2. However, both Lj-TICAM-a and Lj-TICAM-b lack the N-terminal motifs 1–3. The presence of the C-terminal motif 10 in TICAM-1, Lj-TICAM-a, and Bb-TICAM-like suggest that TICAM-1, however recruiting the new N-terminal, is more similar to the ancestor than TICAM-2. And amphioxus Bb-TICAM-like is more similar to Lj-TICAM-a than to Lj-TICAM-b and is likely an ortholog of Lj-TICAM-a.

3.4. Genomic organization of the TICAM gene family

To investigate the changes of *TICAM* gene structure during evolution, a gene structure map was generated, by combining the genetic structure information from the NCBI and the Ensemble website predictions (Fig. 3). Analysis of the genetic structure of the *TICAM* gene family of each species revealed that, while *Lj-TICAM-a* and *Bb-TICAM*-like contain two coding-exons, *Lj-TICAM-b* contains three coding-exons. Therefore, the gene structure of *Bb-TICAM-like* is more similar to that of *Lj-TICAM-a*, which may also indicate that *Lj-TICAM-a* is more likely to be an ortholog of *Bb-TICAM-like* than *Lj-TICAM-b*. In vertebrates, *TICAM-1* and *TICAM-2* contain only one coding-exon, indicating that the gene structure of *Lj-TICAM-a* and *Lj-TICAM-b* changed during evolution, from an original multi-exon structure to a single-exon structure.

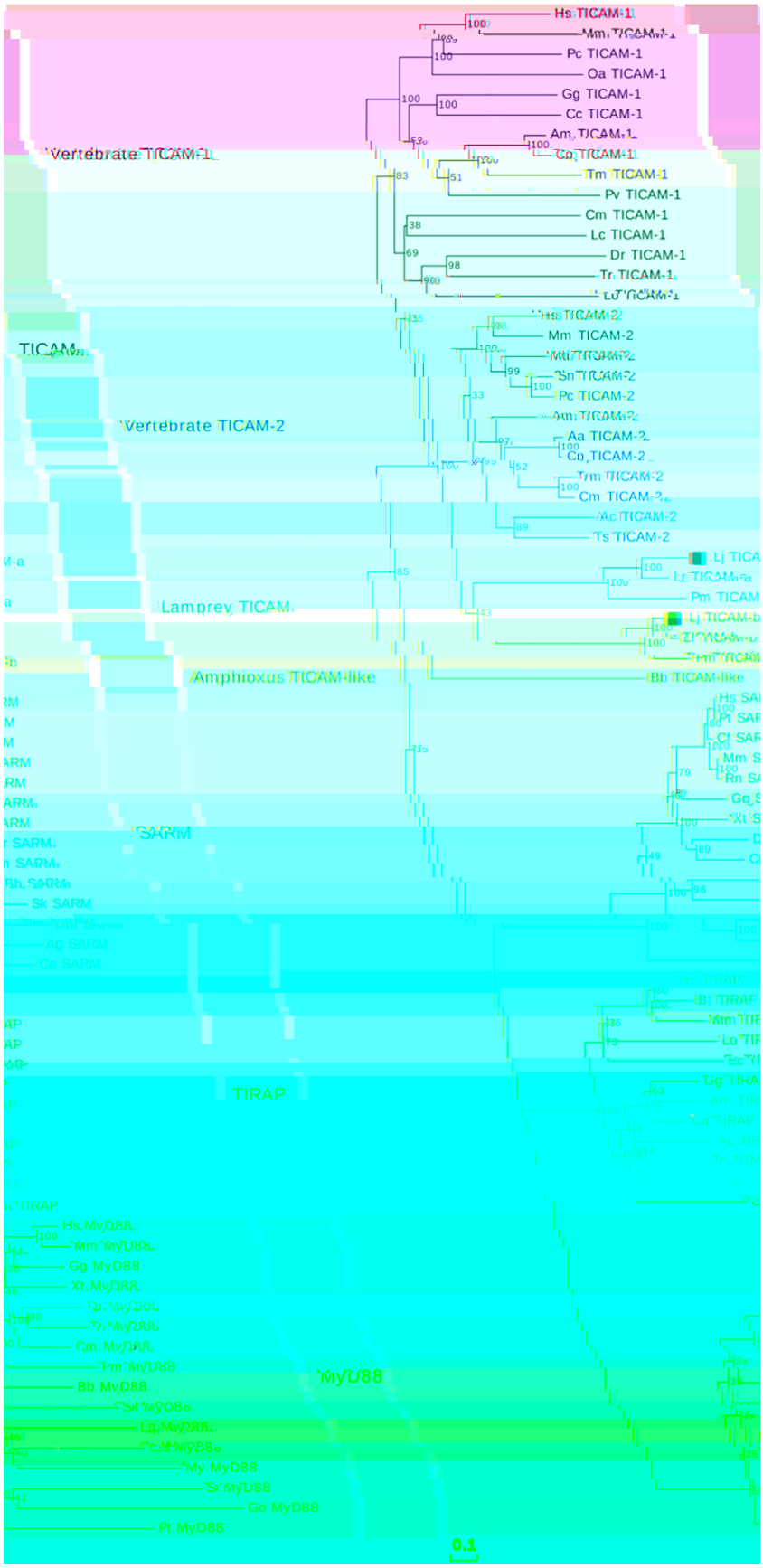

Fig. 1. Phylogenetic tree of TIR-containing adaptors. Evolutionary relationships were calculated based on the full-length protein sequences from all five types of TIR-containing adaptors, including MyD88, SARM, TIRAP/MAL, TICAM-1, and TICAM-2. The bootstrap values labeled at each node show the output from the NJ algorithm. Colored boxes indicate different types of TIR-containing adaptors. See Supplementary Table S1 for all sequences and abbreviations used.

Additionally, the combined length of the exons in *Lj-TICAM-a* was close to the length of the single coding-exon in *Hs-TICAM-1*, suggesting that *TICAM-1* is more conserved than *TICAM-2*. We confirmed the length and location of the introns and exons of *Lj-TICAM-a* and *Lj-TICAM-b* by aligning the coding sequence with the genome sequence. According to the comparative analysis of the two lamprey TICAM sequences, it was found that the third exon of *Lj-TICAM-b* might be copied from the first exon of *Lj-TICAM-a* (Fig. S5). In addition, we found that the main duplication region of *Lj-TICAM-b* is predominantly the TIR domain of *Lj-TICAM-a*.

3.5. Collinearity analysis of the TICAM gene family

Conserved gene neighborhoods in different species can provide information about the phylogenetic relationships between gene family members [47]. Portions of the lamprey *TICAM* were therefore analyzed by comparative genomics (Fig. 4). It has been shown that

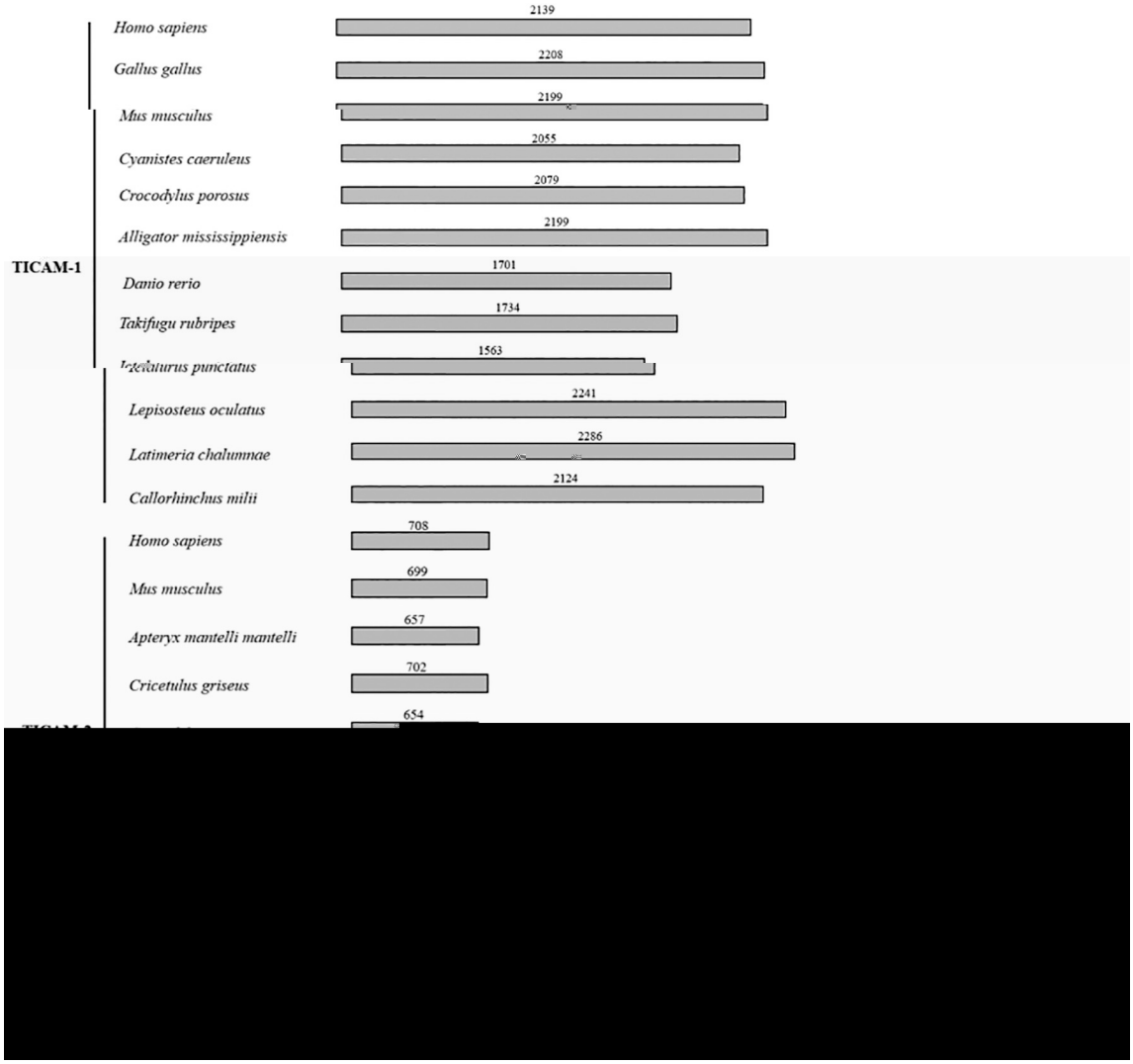

Fig. 3. Comparison of gene structure of *Lj-TICAM-a*, *Lj-TICAM-b*, *Bb-TICAM-like* and their vertebrate counterparts. The genomic organization of *TICAM* genes in different species was compared. The coding-exons and introns are indicated by boxes and lines, respectively. Exon and intron lengths (bp) are shown above the boxes and lines.

Poly I:C, LPS, or PGN, and the temporal expression of the genes in heart tissue was assessed by RT-qPCR (Fig. 5B). Upon stimulation with Poly I: C, the expression of *Lj-TICAM-a* showed a decreasing trend from 0 to 4 h ($P < 0.05$), then peaked at 24 h ($P < 0.05$), and a dropped at 48 h to similar expression at 0 h. Likewise, the expression of *Lj-TICAM-b* in the presence of Poly I:C decreased from 0 to 4 h and increased from 8 to 24 h, illustrating that *Lj-TICAM-a* and *Lj-TICAM-b* shared similar antiviral functions. The expression of *Lj-TICAM-a* and *Lj-TICAM-b* after LPS stimulation did not change significantly but remained relatively stable. Notably, upon PGN stimulation, the expression of *Lj-TICAM-a* remained low from 0 to 8 h, but peaked at 24 h ($P < 0.01$), and decreased at 48 h ($P < 0.05$). In response to PGN stimulation, the expression of *Lj-TICAM-b* increased significantly from 0 to 4 h ($P < 0.05$), decreased from 8 to 24 h, and increased from 48 h ($P < 0.05$). The PGN and Poly I:C challenge had a variable effect on the transcription of *Lj-TICAM-a* and *Lj-TICAM-b* in the heart. TLR molecules recognize specific ligands. Previous studies indicated that TLR3 recognizes Poly I:C whereas TLR2 binds PGN. Therefore, we speculated that TLR3 and TLR2 activated TICAM-dependent signaling pathways, leading to the corresponding effects of Poly I: C and PGN on *Lj-TICAM-a* and *Lj-TICAM-b* transcripts in an immune tissue and in response to Poly I: C and PGN challenge suggested that the two genes have antibacterial and antiviral functions.

3.7. Effect of Lj-TICAM-a and Lj-TICAM-b overexpression on NF-κB promoter activity

TICAM-1 and TICAM-2 are both critical for activating NF-κB or interferon regulatory factors in the mammalian MyD88-independent pathway [10,11]. To test whether Lj-TICAM-a and Lj-TICAM-b performed a similar function, we conducted dual-luciferase assays. Because lamprey cell lines are not available, a human cell line was used for the expression of lamprey genes. The dual-luciferase reporter assays revealed that the activity of the *NF-κB* promoter was not significantly increased in cells transfected with pEGFP-C1-Lj-TICAM-a or pcDNA3.1-N1-HA-Lj-TICAM-b compared with the control group (Fig. 6A and B). Additionally, increasing the dose of pEGFP-C1-Lj-TICAM-a or pcDNA3.1-N1-HA-Lj-TICAM-b used for transfection did not change the *NF-κB* promoter activity. However, the *NF-κB* promoter was activated in cells simultaneously transfected with pEGFP-C1-Lj-TICAM-a and pcDNA3.1-N1-HA-Lj-TICAM-b (Fig. 6C). Increasing the dose of pEGFP-C1-Lj-TICAM-a and pcDNA3.1-N1-HA-Lj-TICAM-b used for transfection slightly weakened the *NF-κB* promoter activity.

3.8. The interaction between Lj-TICAM-a and Lj-TICAM-b

In mammals, TICAM-2 acts as a bridging molecule between TLR4 and TICAM-1 via the interaction of TIR domains, to transmit downstream signals in the pathway [48], indicating that TICAM-1 and TICAM-2 interact in mammals. Accordingly, co-immunoprecipitation was used to verify whether Lj-TICAM-a and Lj-TICAM-b interact to activate the *NF-κB* promoter (Fig. 6D). Western blot analysis showed that Lj-TICAM-a and Lj-TICAM-b were present in whole-cell lysates, confirming their overexpression. Moreover, Lj-TICAM-a was detected in the precipitate, indicating that Lj-TICAM-a and Lj-TICAM-b interacted to form a complex for function.

3.9. Effect of Lj-TICAM-a and Lj-TICAM-b overexpression on the NF-κB signaling pathway

The dual luciferase assay showed that simultaneous overexpression of pEGFP-C1-LjTICAM-a and pcDNA3.1-N1-HA-LjTICAM-b could activate NF-κB. We sought to verify the effect of lamprey TICAM on the NF-κB signaling pathway at the protein level (Fig. 6E). Gray value analysis of the protein expression between the empty vector and the experimental groups, revealed that the levels of phospho-IKB (Ser32/Ser36), NF-κB-p65, and phospho-NF-κB-p65 (Ser536) protein were significantly up-regulated (Fig. 6F), further showing that Lj-TICAM-a and Lj-TICAM-b could activate the NF-κB signaling pathway by forming a complex. Moreover, analysis of the changes in the expression of TRAF3 and TRAF6, which are the key molecules in the downstream of the TICAM-mediated signaling pathway showed that, different from mammalians, the lamprey TICAM-dependent signaling pathway might rely on TRAF3 rather than on TRAF6 (Fig. 6F).

4. Discussion

In the current study, we used comparative genomics and molecular evolution analysis to investigate the origin and evolutionary history of Lj-TICAM-a and Lj-TICAM-b. We also analyzed the functional characteristics of Lj-TICAM-a and Lj-TICAM-b, and their functional differentiation after gene duplication.

4.1. Origin and evolution of Lj-TICAM-a and

Lamprey occupies

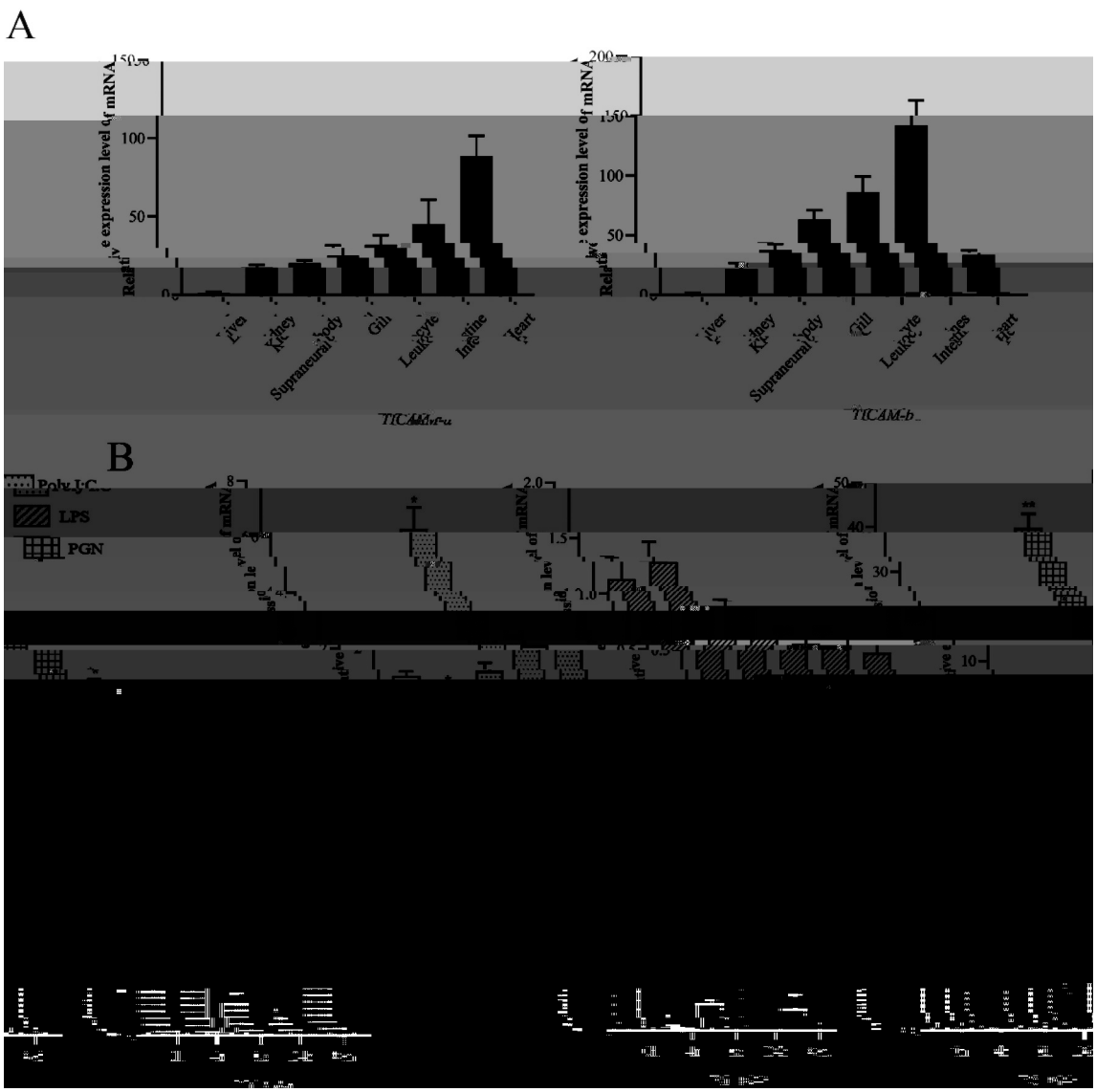

Fig. 5. Expression of *TICAM-a* and *TICAM-b* in L. *japonica*. (A) Expression of *Lj-TICAM-a* and *Lj-TICAM-b* in different lamprey tissues, as determined by RT-qPCR. (B) Expression of *Lj-TICAM-a* and *Lj-TICAM-b* in the heart upon stimulation by Poly I:C, LPS, and PGN. Gene expression levels were normalized to *GAPDH* expression. Statistics are shown by asterisks. Values are expressed as the mean ± SD ($n = 3$), with bars representing the standard error. *P < 0.05, **P < 0.01.

amphioxus TICAM-like is located at the root of vertebrate TICAM clade, suggesting that it may be the ancestors of the lamprey TICAM (Fig. 1). Furthermore, motif and gene structure analysis indicate that Bb-TICAM-like is more similar to Lj-TICAM-a than to Lj-TICAM-b (Figs. 2 and 3). The monophyletic clustering of lamprey TICAM-a and TICAM-b in the phylogenetic tree suggests that these genes were derived from a specific duplication event. Because the hagfish only contains *TICAM-a*, *Lj-TICAM-b* most likely arose from *Lj-TICAM-a* via species-specific tandem duplication (Fig. 4).

There are many speculations on the evolutionary relationship between Lj-TICAM-a and Lj-TICAM-b and vertebrate TICAM-1 and TICAM-2. The phylogenetic trees and motif analysis in the current study suggest that *Lj-TICAM-a* and *Lj-TICAM-b* are the ancestral gene of the vertebrate *TICAM* genes (Fig. 1). Unlike the single-exon vertebrate *TICAM-1* and *TICAM-2* genes, *Lj-TICAM-a* and *Lj-TICAM-b* are both multi-exon genes (Fig. 3). This indicates that intron-loss events, which are mostly mediated through retrotransposition, might have occurred during the evolutionary history of the vertebrate *TICAM* family. Multiple-sequence alignments reveal that Lj-TICAM-a and Lj-TICAM-b are both more similar to TICAM-1 than to TICAM-2 (Fig. S4). Motif structures, in addition to the exon lengths, also indicate vertebrate TICAM-1 is more primitive and more similar to the common ancestor than vertebrate TICAM-2 (Figs. 2 and 3). This observation led us to hypothesize that *Lj-TICAM-a* is a direct ancestral gene of vertebrate *TICAM-1*.

The mammalian *TICAM-1* and *TICAM-2* genes are thought to have undergone two rounds of WGD early in the evolution [19,22]. It is commonly assumed that the two molecules evolved independently in vertebrates, but no explanation has been given for the appearance of the two genes in lamprey. In the early vertebrate, *TICAM-1* was evolutionarily conserved [21], and homologs of *TICAM-2* have not been identified in teleosts [52,53], *Xenopus* [54], or chicken [55], but have been found in mammals and shark. Combined with the theory of 2R occurring at the origin of vertebrates and the first round of WGD occurring before the emergence of agnathans [29,56], we speculated that *Lj-TICAM-a* survived through the first round of WGD, while *Lj-TICAM-b* originated after a species-specific tandem repeat event via *Lj-TICAM-a* duplication. Since the ortholog of vertebrate *TICAM-2* was not identified in lamprey, it is likely that *TICAM-2* arose from *TICAM-1* via duplication (WGD) very shortly after the split of jawless and jawed vertebrates and first appeared in shark. We propose a model for the evolution of *Lj-TICAM-a* into

TICAM-1, in which *Lj-TICAM-a* was inserted into another chromosomal segment upstream of *FEM1* by retrotransposition to form a single-exon structure, and a new 5′-flanking sequence was recruited to produce *TICAM-1*, while *TICAM-2* was formed by a segmental duplication of the primitive *TICAM-1–FEM1* locus or the second round of WGD (Fig. 7).

4.2. Functional divergence of Lj-TICAM-a and Lj-TICAM-b

Expression analysis revealed similar expression of *Lj-TICAM-a* and *Lj-TICAM-b* in various tissues (Fig. 4A). Furthermore, the expression of these genes was not affected by LPS stimulation (Fig. 4B), implying their functional similarity. Studies of the TLR signaling pathway have identified Poly I:C and PGN as TLR3 and TLR2 ligands, respectively [57]. Recently, it was reported that fish TRIF responds to PGN stimulation [58,59]. We observed that PGN injection stimulated *Lj-TICAM-a* and *Lj-TICAM-b* expression to varying degrees, which has not been observed in o ed

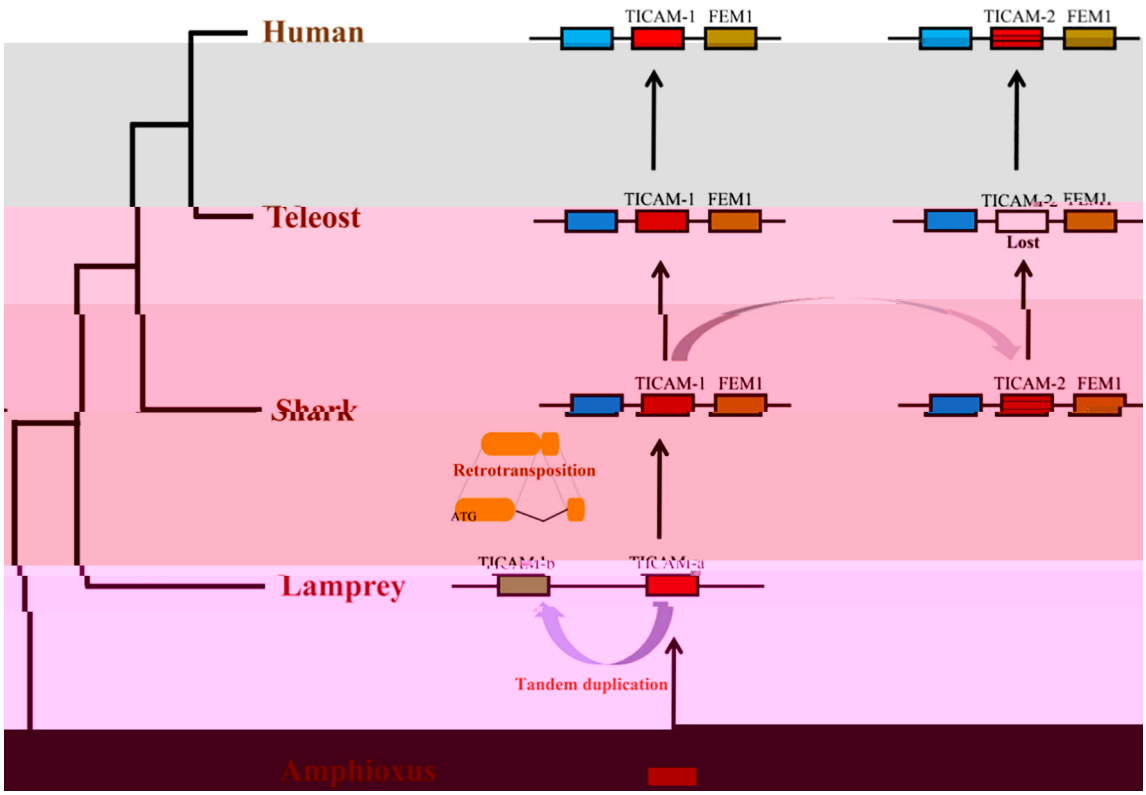

Fig. 7. Model for the historical relationships of *TICAM* genes. *TICAM-like* gene from ancient Cephalochordata is shown as a common ancestor of *TICAM* genes. After the first round of WGD (1R), *Lj-TICAM-a* surivided and partially tandem duplicated to *Lj-TICAM-b*. Following retrotransposition and recruiting the new 5′-flanking sequence, *TICAM-1* appeared and formed *TICAM-2* in shark. *TICAM-2* was later lost by non-mammalian vertebrates during evolution. Finally, *TICAM-2* was retrieved by mammals.

downstream molecules by forming a complex. It was also confirmed that *Lj-TICAM-b* is not a pseudogene duplicated by *Lj-TICAM-a* and that this gene has evolved different functions likely through neofunctionalization or sub-functionalization.

The evolutionary history of TLR-mediated signaling networks provides essential insights into the origin and diversification of the vertebrate immune system. We provide a picture of the origin and evolution of the lamprey TICAM family and reveal the important roles of lamprey-specific gene duplication and subsequent functional divergence in immune system evolution. However, the underlying functional divergence mechanism and evolutionary driving forces require further analysis. Particularly, the details of TICAM-dependent TLR signaling pathways in the lamprey antiviral response remain unclear. Further investigation of the lamprey TLR pathway may provide insight into vertebrate antiviral immunology and drug development.

Funding

This work was supported by the grants from the National Natural Science Foundation of China (No. 31601044), the China Postdoctoral Science Foundation (2016M591454), the Scientific Research Foundation of the Higher Education Institutions of Liaoning Province, China (No. LQ2020025), the High Lever Talent Innovation Support Project from Dalian to Ting Zhu, and the Undergraduate Innovation and Entrepreneurship Training Program Support Project (S202010165041).

Acknowledgments

We would like to thank Editage (www.editage.cn) for English language editing.

Appendix A. Supplementary data

Supplementary data to this article can be found online at https://doi.org/10.1016/j.ygeno.2021.06.022.

References

[1] E. Meylan, J. Tschopp, M. Karin, Intracellular pattern recognition receptors in the host response, Nature. 442 (2006) 39–44, https://doi.org/10.1038/nature04946.
[2] T. Kawai, S. Akira, The roles of TLRs, RLRs and NLRs in pathogen recognition, Int. Immunol. 21 (2009) 317–337, https://doi.org/10.1093/intimm/dxp017.
[3] T.H. Mogensen, Pathogen recognition and inflammatory signaling in innate immune defenses, Clin. Microbiol. Rev. 22 (2009) 240–273, https://doi.org/10.1128/CMR.00046-08.
[4] T. Kawai, S. Akira, The role of pattern-recognition receptors in innate immunity: update on toll-like receptors, Nat. Immunol. 11 (2010) 373–384, https://doi.org/10.1038/ni.1863.
[5] L.A. O Neill, A.G. Bowie, The family of five: TIR-domain-containing adaptors in toll-like receptor signalling, Nat. Rev. Immunol. 7 (2007) 353–364, https://doi.org/10.1038/nri2079.
[6] M.O. Ullah, M.J. Sweet, A. Mansell, S. Kellie, B. Kobe, TRIF-dependent TLR signaling, its functions in host defense and inflammation, and its potential as a therapeutic target, J. Leukoc. Biol. 100 (2016) 27–45, https://doi.org/10.1189/jlb.2RI1115-531R.
[7] S. Akira, K. Takeda, T. Kaisho, Toll-like receptors: critical proteins linking innate and acquired immunity, Nat. Immunol. 2 (2001) 675–680, https://doi.org/10.1038/90609.
[8] J. Peng, Q.A. Yuan, B. Lin, P. Panneerselvam, X.W. Wang, X.L. Luan, S.K. Lim, B. P. Leung, B. Ho, J.L. Ding, SARM inhibits both TRIF and MyD88 mediated AP-1 activation, Eur. J. Immunol. 40 (2010) 1738–1747, https://doi.org/10.1002/eji.200940034.
[9] T. Horng, G.M. Barton, R.A. Flavell, R. Medzhitov, The adaptor molecule TIRAP provides signalling specificity for toll-like receptors, Nature. 420 (2002) 329–333, https://doi.org/10.1038/nature01180.
[10] M. Yamamoto, S. Sato, H. Hemmi, H. Sanjo, S. Uematsu, T. Kaisho, K. Hoshino, O. Takeuchi, M. Kobayashi, T. Fujita, K. Takeda, S. Akira, Essential role for TIRAP in activation of the signalling cascade shared by TLR2 and TLR4, Nature. 420 (2002) 324–329, https://doi.org/10.1038/nature01182.

[11] H. Oshiumi, M. Matsumoto, K. Funami, T. Akazawa, T. Seya, TICAM-1, an adaptor molecule that participates in toll-like receptor 3-mediated interferon beta induction, Nat. Immunol. 4 (2003) 161–167, https://doi.org/10.1038/ni886.
[12] H. Oshiumi, M. Matsumoto, K. Funami, T. Akazawa, T. Seya, TIR-containing adapter molecule (TICAM)-2, a bridging adapter recruiting to toll-like receptor 4 TICAM-1 that induces interferon-beta, J. Biol. Chem. 278 (2003) 49751–49762, https://doi.org/10.1074/jbc.M305820200.
[13] K.A. Jenkins, A. Mansell, TIR-containing adaptors in toll-like receptor signalling, Cytokine. 49 (2010) 237–244, https://doi.org/10.1016/j.cyto.2009.01.009.
[14] H. Kumar, T. Kawai, S. Akira, Toll-like receptors and innate immunity, Biochem. Biophys. Res. Commun. 388 (2009) 621–625, https://doi.org/10.1016/j.bbrc.2009.08.062.
[15] S. Sato, M. Sugiyama, M. Yamamoto, Y. Watanabe, T. Kawai, K. Takeda, S. Akira, Toll/IL-1 receptor domain-containing adaptor inducing IFN-beta (TRIF) associates with TNF receptor-associated factor 6 and TANK-binding kinase 1, and activates two distinct transcription factors, NF-kappa B and IFN-regulatory factor-3, in the toll-like receptor signaling, J. Immunol. 171 (2003) 4304–4310, https://doi.org/10.4049/jimmunol.171.8.4304.
[16] J. Gohda, T. Matsumura, J. Inoue, Cutting edge: TNFR-associated factor (TRAF) 6 is essential for MyD88-dependent pathway but not toll/IL-1 receptor domain-containing adaptor-inducing IFN-beta (TRIF)-dependent pathway in TLR signaling, J. Immunol. 173 (2004) 2913–2917, https://doi.org/10.4049/jimmunol.173.5.2913.
[17] V. Häcker, B. Redecke, I. Blagoev, L.C. Kratchmarova, G.G. Hsu, M.P. Kamps Wang, E. Raz, H. Wagner, G. Häcker, M. Mann, M. Karin, Specificity in Toll-like receptor signalling through distinct effector functions of TRAF3 and TRAF6, Nature 439 (2006) 204–207, https://doi.org/10.1038/nature04369.
[18] G. Oganesyan, S.K. Saha, B. Guo, J.Q. He, A. Shahangian, B. Zarnegar, A. Perry, G. Cheng, Critical role of TRAF3 in the Toll-like receptor-dependent and independent antiviral response, Nature 439 (2006) 208–211, https://doi.org/10.1038/nature04374.
[19] C. Sullivan, J.H. Postlethwait, C.R. Lage, P.J. Millard, C.H. Kim, Evidence for evolving toll-IL-1 receptor-containing adaptormolecule function in vertebrates, J. Immunol. 178 (2007) 4517–4527, https://doi.org/10.4049/jimmunol.178.7.4517.
[20] S. Fan, S. Chen, Y. Liu, Y. Lin, H. Liu, L. Guo, B. Lin, S. Huang, A. Xu, Zebrafish TRIF, a Golgi-localized protein, participates in IFN induction and NF-kappaB activation, J. Immunol. 180 (2008) 5373–5383, https://doi.org/10.4049/jimmunol.180.8.5373.
[21] T. Seya, M. Matsumoto, T. Ebihara, H. Oshiumi, Functional evolution of the TICAM-1 pathway for extrinsic RNA sensing, Immunol. Rev. 227 (2009) 44–53, https://doi.org/10.1111/j.1600-065X.2008.00723.x.
[22] B. Wu, B. Xin, M. Jin, T. Wei, Z. Bai, Comparative and phylogenetic analyses of three TIR domain-containing adaptors in metazoans: implications for evolution of TLR signaling pathways, Dev. Comp. Immunol. 35 (2011) 764–773, https://doi.org/10.1016/j.dci.2011.02.009.
[23] M. Yang, S. Yuan, S. Huang, J. Li, L. Xu, H. Huang, X. Tao, J. Peng, A. Xu, Characterization of bbtTICAM from amphioxus suggests the emergence of a MyD88-independent pathway in basal chordates, Cell Res. 21 (2011) 1410–1423, https://doi.org/10.1038/cr.2011.156.
[24] H. Kaessmann, Origins, evolution, and phenotypic impact of new genes, Genome Res. 20 (2010) 1313–1326, https://doi.org/10.1101/gr.101386.109.
[25] M. Lynch, J.S. Conery, The evolutionary fate and consequences of duplicate genes, Science. 290 (2000) 1151–1155, https://doi.org/10.1126/science.290.5494.1151.
[26] V.E. Prince, F.B. Pickett, Splitting pairs: the diverging fates of duplicated genes, Nat. Rev. Genet. 3 (2002) 827–837, https://doi.org/10.1038/nrg928.
[27] L. Man, B. Esther, T. Kevin, W. Wen, The origin of new genes: glimpses from the young and old, Nat. Rev. Genet. 4 (2003) 865–875, https://doi.org/10.1038/nrg1204.
[28] D. Yun, Z. Qi, W. Wen, Origins of new genes and evolution of their novel functions, Annu. Rev. Ecol. Evol. Syst. 43 (2012) 345–363.
[29] P. Dehal, J.L. Boore, Two rounds of whole genome duplication in the ancestral vertebrate, PLoS Biol. 3 (2005), e314, https://doi.org/10.1371/journal.pbio.0030314.
[30] M. Kasahara, Genome duplication and T cell immunity, Prog. Mol. Biol. Transl. Sci. 92 (2010) 7–36, https://doi.org/10.1016/S1877-1173(10)92002-4.
[31] L.Z. Holland, D. Ocampo Daza, A new look at an old question: when did the second whole genome duplication occur in vertebrate evolution? Genome Biol. 19 (2018) 209, https://doi.org/10.1186/s13059-018-1592-0.
[32] S. Kuraku, A. Meyer, S. Kuratani, Timing of genome duplications relative to the origin of the vertebrates: did cyclostomes diverge before or after? Mol. Biol. Evol. 26 (2009) 47–59, https://doi.org/10.1093/molbev/msn222.
[33] C. Sacerdot, A. Louis, C. Bon, C. Berthelot, H. Roest Crollius, Chromosome evolution at the origin

3

[60] P. Baoprasertkul, E. Peatman, B. Somridhivej, Z. Liu, Toll-like receptor 3 and TICAM genes in catfish: species-specific expression profiles following infection with *Edwardsiella ictaluri*, Immunogenetics. 58 (2016) 817–830, https://doi.org/10.1007/s00251-006-0144-z.

[61] J. Wei, X. Zhang, S. Zang, Q. Qin, Expression and functional characterization of TRIF in orange-spotted grouper (*Epinephelus coioides*), Fish Shellfish Immunol. 71 (2017) 295–304, https://doi.org/10.1016/j.fsi.2017.09.063.

[62] E.H. Hwang, T.H. Kim, S.M. Oh, K.B. Lee, S.J. Yang, J.H. Park, Toll/IL-1 domain-containing adaptor inducing IFN-β (TRIF) mediates innate immune responses in murine peritoneal mesothelial cells through TLR3 and TLR4 stimulation, Cytokine. 77 (2016) 127–134, https://doi.org/10.1016/j.cyto.2015.11.010.

[63] J.C. Kagan, T. Su, T. Horng, A. Chow, S. Akira, R. Medzhitov, TRAM couples endocytosis of toll-like receptor 4 to the induction of interferon-beta, Nat. Immunol. 9 (2008) 361–368, https://doi.org/10.1038/ni1569.

[64] M.G. Tassia, N.V. Whelan, K.M. Halanych, Toll-like receptor pathway evolution in deuterostomes, Proc. Natl. Acad. Sci. U. S. A. 114 (2017) 7055–7060, https://doi.org/10.1073/pnas.1617722114.

[65] K.A. Fitzgerald, J.C. Kagan, Toll-like receptors and the control of immunity, Cell. 180 (2020) 1044–1066, https://doi.org/10.1016/j.cell.2020.02.041.

[66] G.V. Ermakova, A.V. Kucheryavyy, A.G. Zaraisky, A.V. Bayramov, Discovery of four noggin genes in lampreys suggests two rounds of ancient genome duplication, Commun. Biol. 3 (2020) 501.

[67] J.J. Smith, N. Timoshevskaya, C. Ye, C. Holt, M.C. Keinath, H.J. Parker, M.E. Cook, J.E. Hess, S.R. Narum, F. Lamanna, H. Kaessmann, V.A. Timoshevskiy, C.K. M. Waterbury, C. Saraceno, L.M. Wiedemann, S.M.C. Robb, C. Baker, E.E. Eichler, D. Hockman, T. Sauka-Spengler, M. Yandell, R. Krumlauf, G. Elgar, C.T. Amemiya, The sea lamprey germline genome provides insights into programmed genome rearrangement and vertebrate evolution, Nat. Genet. 50 (2018) 270–277.